

---

# JOURNAL OF THE AMERICAN CHEMICAL SOCIETY

---

## Free Energy Perturbation Studies on Inhibitor Binding to HIV-1 Proteinase

B. G. Rao,<sup>†</sup> R. F. Tilton,<sup>‡</sup> and U. C. Singh\*

*Contribution from the Department of Molecular Biology, Scripps Clinic and Research Foundation, La Jolla, California 92037, and Department of Structural Chemistry, Miles Research Center, West Haven, Connecticut 06516. Received November 1, 1991*

**Abstract:** The free energy perturbation method has been employed to determine the binding free energy contributions of different groups of two classes of HIV-1 proteinase inhibitors: (1) a hydroxyethylene isostere inhibitor, Ala-Ala-Phe[CH(OH)-CH<sub>2</sub>]Gly-Val-Val-OMe (reported by Dreyer et al.<sup>1</sup>), and a reduced peptide inhibitor, MVT-101 (reported by Miller et al.<sup>2</sup>). For the first inhibitor, the configuration of the central hydroxyl group is changed from *S* to *R* in two steps. In the first step, the hydroxyl group in the *S* configuration was mutated to a hydrogen, and in the second step, the hydroxyl group of the (*R*)-OH analogue of the inhibitor was mutated to a hydrogen. In this way the binding contributions of the hydroxyl group in the two diastereomers are determined separately in addition to obtaining the effect of changing the hydroxyl group configuration from *S* to *R*. The calculated free energy difference between the binding of the two diastereomers is  $3.37 \pm 0.64$  kcal/mol, which is close to the experimental value of 2.6 kcal/mol. The calculations on the substitution of Gly by Nle at the P<sub>1</sub> position of the same inhibitor predict an enhancement in the binding by about 1.7 kcal/mol. Similar calculations on the substitution of Nle with Met in MVT-101 inhibitor predict a decrease in binding by about 0.7 kcal/mol. The details of these results will be discussed and compared with the results of a similar study on pepstatin-*rhizopus* pepsin complex.

### Introduction

Several tight-binding inhibitors of human immunodeficiency virus type 1 proteinase (HIV-1 PR) have been discovered as potential drugs against AIDS by modification of the scissile P<sub>1</sub>-P<sub>1</sub> peptide bond of enzyme substrates by peptidomimetics, like statine, hydroxyethylene, and hydroxyethylamine etc.<sup>3</sup> HIV-1 PR is an aspartic proteinase which is active as a dimer with each monomer having 99 amino acid residues. An important structural feature of the inhibitors of this enzyme is a hydroxyl group which hydrogen bonds to the carboxylates of the catalytically important Asp diad in the middle of the enzyme active site.<sup>4</sup> Such a structural feature is also present in most tight-binding inhibitors of non-viral aspartic proteinases.<sup>5</sup> Except in a few cases,<sup>6,7</sup> the *S* configuration is preferred at the chiral center bearing the hydroxyl group. The *S* diastereomer of an HIV-1 PR inhibitor binds about 80 times better than the *R* diastereomer, which is equivalent to a binding free energy difference of about 2.6 kcal/mol between the two

diastereomers.<sup>1,7</sup> The difference in binding free energies of the two diastereomers of pepstatin to porcine pepsin is much larger (about

---

(1) Dreyer, G. B.; Metcalf, B. W.; Tomaszek, T. A., Jr.; Carr, T. J.; Chandler, A. C., III; Hyland, L.; Fakhoury, S. A.; Maggaard, V. W.; Moore, M. L.; Strickler, J. E.; Debouck, C.; Meek, T. D. *Proc. Natl. Acad. Sci. U.S.A.* **1989**, *86*, 9752.

(2) Miller, M.; Schneider, J.; Sathyanarayana, B. K.; Toth, M. V.; Marshall, G. R.; Clawson, L.; Selk, L.; Kent, S. B. H.; Wlodawer, A. *Science* **1989**, *246*, 1149.

(3) For a recent review, see: Huff, J. R. *J. Med. Chem.* **1991**, *34*, 2305.

(4) (a) Fitzgerald, P. M. D.; McKeever, B. M.; VanMiddlesworth, J. F.; Springer, J. P.; Heimback, J. C.; Leu, C.; Herber, W. K.; Dixon, R. A.; Drake, P. L. *J. Biol. Chem.* **1990**, *265*, 14209. (b) Swain, A. L.; Miller, M. M.; Green, J.; Rich, D. H.; Schneider, J.; Kent, S.; Wlodawer, A. *Proc. Natl. Acad. Sci. U.S.A.* **1990**, *87*, 8805. (c) Jaskolski, M.; Tomaselli, A. G.; Sawyer, T. K.; Staples, D. G.; Heinrichson, R. L.; Schneider, J.; Kent, S. B. H.; Wlodawer, A. *Biochemistry* **1991**, *30*, 1600.

(5) For a review, see: Davies, D. R. *Annu. Rev. Biophys. Biophys. Chem.* **1990**, *19*, 189.

(6) Roberts, N. A.; Martin, J. A.; Kinchington, D.; Broadhurst, A. V.; Craig, J. C.; Duncan, I. B.; Galpin, S. A.; Handa, B. K.; Kay, J.; Krohn, A.; Lambert, R. W.; Merrett, J. H.; Mills, J. S.; Parkes, K. E. B.; Redshaw, S.; Ritchie, A. J.; Taylor, D. L.; Thomas, G. I.; Machin, P. J. *Science* **1990**, *248*, 358.

---

\* Address correspondence to this author at Scripps Clinic and Research Foundation.

<sup>†</sup> Present Address: Vertex Pharmaceuticals Inc., Cambridge, MA 02139.

<sup>‡</sup> Miles Research Center.

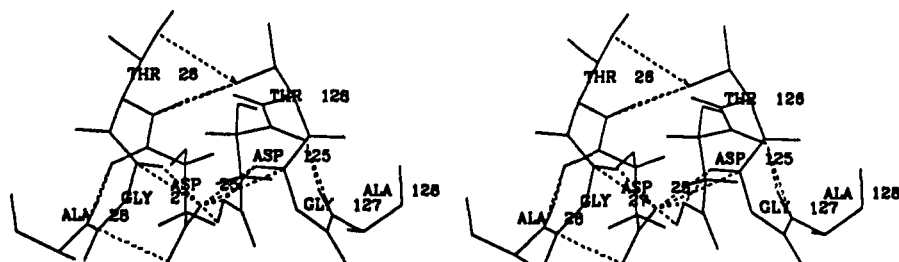


**Figure 1.** Structure of the active site Asp diad and the neighboring residues in the crystal structure of HIV-1 proteinase (4HVP structure). One of the Asp residues (Asp-125) is neutral in this structure.

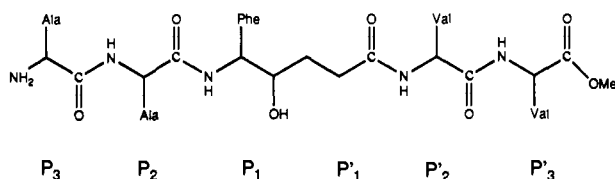


**Figure 2.** Structure of HEI, the hydroxyethylene inhibitor. The residues are labeled (P<sub>3</sub>-P'<sub>3</sub>) from the amino to carboxyl terminus.

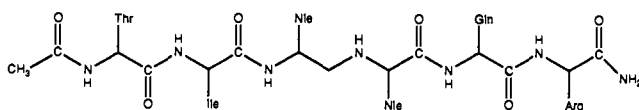
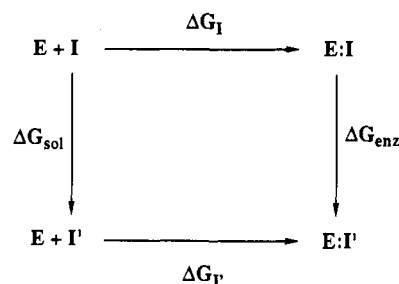


**Figure 3.** Structure of MVT-101. Nle represents norleucine.

5.0 kcal/mol).<sup>8</sup> It appears that the inhibitor binding to HIV-1 PR is less stereospecific compared to non-viral aspartic proteinases. This may be due to the differences in the interactions between these two types of enzymes with their inhibitors as seen in the structures of the enzyme-inhibitor complexes.<sup>4,5</sup>

Though the structures of the viral and non-viral aspartic proteinases are similar in most respects, there are some important differences in the hydrogen bonding around the Asp diad at the center of the active site. The hydrogen-bonding interaction between the Asp diad and the neighboring residues of HIV-1 PR is shown in Figure 1. It may be noted that the fourth residue following Asp-25 is Ala in HIV-1 PR, whereas it is either Ser or Thr in pepsins,<sup>9</sup> and the side chain OH groups of these residues hydrogen bond to the outer oxygens of the two Asp carboxylates. The absence of such hydrogen bond interactions in HIV-1 PR active site may result in a more flexible and basic Asp side chain compared to the side chains of Asp diad in the pepsins. It is of interest to determine if these structural differences are responsible for the different binding free energies for the two classes of enzyme-inhibitor complexes.

The free energy perturbation method<sup>10</sup> is an advanced computer simulation technique suitable for studying differences in binding of closely related enzyme inhibitors. We have recently investigated<sup>11</sup> pepstatin binding with *rhizopus* pepsin using this method. We have found that the free energy of binding of pepstatin increases by about 5.0 kcal/mol when the configuration of the hydroxyl group of the central statine residue is changed from *S* to *R*. The same effect is observed when the (*S*)-hydroxyl group is changed to a hydrogen. A similar study is reported here on binding of a hydroxyethylene isostere inhibitor HEI<sup>1</sup> (shown in Figure 2) to HIV-1 PR to understand the differences in inhibitor binding between the HIV-1 PR and the non-viral cellular aspartic



$$\Delta\Delta G_{\text{bind}} = \Delta G_{1'} - \Delta G_1 = \Delta G_{\text{enz}} - \Delta G_{\text{sol}}$$

**Figure 4.** The thermodynamic cycle used in the computation of  $\Delta\Delta G_{\text{bind}}$ .

proteinases. Additionally, another mutation was carried out to predict the effect of an obvious modification on this inhibitor. A comparison of the inhibitor HEI and a reduced peptide inhibitor MVT-101<sup>2</sup> (shown in Figure 3) shows that the inhibitor HEI lacks the side chain to fill the S'<sub>1</sub> pocket of the enzyme. This pocket is hydrophobic and similar in size to the S<sub>1</sub> pocket, and hence it is obvious that a hydrophobic side chain at the P'<sub>1</sub> position on the inhibitor HEI will enhance its binding. We have simulated an addition of a norleucine (Nle) side chain at this position and calculated the change in its free energy of binding. The side chain of Nle consists of an *n*-butyl group. A free energy simulation on MVT-101 inhibitor was carried out to estimate the effect of a mutation of Nle to Met at the P<sub>1</sub> and P'<sub>1</sub> sites on the unmodified substrate of this enzyme. This mutation is achieved by changing the CH<sub>2</sub> group at the  $\delta$  position of the Nle side chain into a sulfur atom.

**The Free Energy Perturbation Method.** In the free energy perturbation approach,<sup>10</sup> the free energy difference between two states of a system is computed by transforming one state into the other by changing a single coupling parameter in several steps. For instance, the two states, A and B represented by Hamiltonians  $H_A$  and  $H_B$ , are coupled by a dimensionless parameter,  $\lambda$ , as

$$H_\lambda = \lambda H_A + (1 - \lambda) H_B \quad 0 \leq \lambda \leq 1 \quad (1)$$

When  $\lambda = 1$ ,  $H_\lambda = H_A$ , and when  $\lambda = 0$ ,  $H_\lambda = H_B$ . Therefore, state A can be smoothly transformed to state B by changing the value of  $\lambda$  in small increments,  $\Delta\lambda$ , such that the system is in equilibrium at all values of  $\lambda$ . At intermediate values of  $\lambda$ , the state is a hypothetical mixture of A and B.

The Gibbs free energy change due to the perturbation at  $\lambda$  is given by

$$\Delta G_{\lambda_i} = -\frac{1}{\beta} \ln \langle \exp(-\beta \Delta H_{\lambda_i}) \rangle_0 \quad (2)$$

where  $\beta = 1/RT$ . The average of  $\exp(-\beta \Delta H_{\lambda_i})$  is computed over the unperturbed ensemble of the system. If the perturbation from  $\lambda_1 = 1$  to  $\lambda_N = 0$  is carried over  $N$  intervals, then the total free energy change equals the sum over all these intervals

$$\Delta G = \sum_{i=1}^N \Delta G_{\lambda_i} \quad (3)$$

It is standard practice to make use of the thermodynamic cycle<sup>11-14</sup> described in Figure 4 to determine the difference in the

(7) Rich, D. H.; Sun, C. Q.; Vara Prasad, J. V. N.; Pathiaseril, A.; Toth, M. V.; Marshall, G. R.; Clare, M.; Mueller, R. A.; Houseman, K. *J. Med. Chem.* **1991**, *34*, 1222.

(8) Rich, D. H. *J. Med. Chem.* **1985**, *28*, 263.

(9) For renin, one of these residues is Ser and the other is Ala.

(10) For recent reviews on free energy perturbation calculations, see: (a) Beveridge, D. L.; DiCupa, F. M. *Annu. Rev. Biophys. Biophys. Chem.* **1989**, *18*, 431. (b) van Gunsteren, W. F. *Protein Eng.* **1988**, *2*, 5. (c) Richards, W. G.; King, P. M.; Reynolds, C. A. *Protein Eng.* **1989**, *2*, 319. (d) Jorgensen, W. L. *Acc. Chem. Res.* **1989**, *22*, 184. (e) Kollman, P. A.; Merz, K. M., Jr. *Acc. Chem. Res.* **1990**, *23*, 246; *Engl. Ed.* **1990**, *29*, 992. (f) Karplus, M.; Petsko, G. A. *Nature* **1990**, *347*, 631.

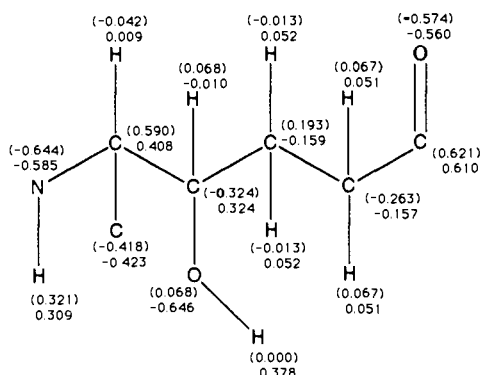


Figure 5. Charges on the hydroxyethylene core of HEI. The values in parentheses are the charges of the dehydroxy (or ethylene) core, which is the end state of the hydroxyl group mutation.

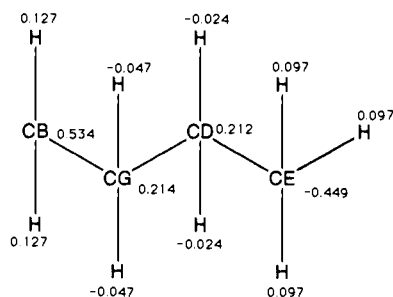


Figure 6. Charges on the norleucine (Nle) side chain.

free energy of binding,  $\Delta\Delta G_{\text{bind}}$ , between any two inhibitors, I and I', with an enzyme, E. In this figure,  $\Delta G_I$  and  $\Delta G_{I'}$  represent the free energies of binding of inhibitors I and I', respectively. Further,  $\Delta G_{\text{sol}}$  represents the difference between the solvation free energies of the two inhibitors, and the difference in the free energies of binding of the two inhibitors in the enzyme active site is represented by  $\Delta G_{\text{enz}}$ . Since free energy is a state function, it is possible to write the following equation from the consideration of the scheme in Figure 4.

$$\Delta\Delta G_{\text{bind}} = \Delta G_{I'} - \Delta G_I = \Delta G_{\text{enz}} - \Delta G_{\text{sol}} \quad (4)$$

It is straightforward and easier to determine  $\Delta G_{\text{enz}}$  and  $\Delta G_{\text{sol}}$  terms compared to  $\Delta G_I$  and  $\Delta G_{I'}$  terms. Therefore,  $\Delta G_{\text{enz}}$  and  $\Delta G_{\text{sol}}$  terms are determined by mutating one inhibitor into another in the active site of the enzyme and in water respectively in two separate simulations to compute  $\Delta\Delta G_{\text{bind}}$ .

### Computational Details

For molecular mechanics, molecular dynamics, and free energy perturbation calculations, AMBER (3.3) programs<sup>15</sup> were used. A united atom model representation of the AMBER forcefield<sup>16</sup> was used for the enzyme residues. For the inhibitor and the two active site Asp residues, the all atom model was used. The partial charges for the novel amino acids and the inhibitor groups were determined with the QUEST program<sup>17</sup> by the electrostatic potential fit method.<sup>18</sup> The electrostatic potentials were generated by the ab initio method using the 6-31G\* basis set. The

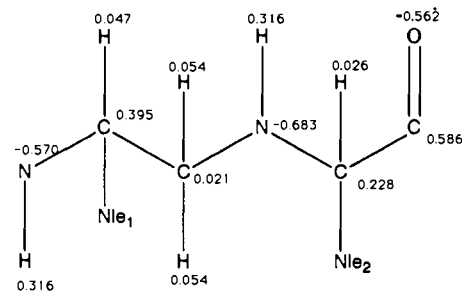


Figure 7. Charges on the reduced peptide core of MVT-101.

Table I. The Mutation Results on the Inhibitors in Water

no.	inhibitor	mutation	time, ps	$\Delta G_{\text{sol}}^a$
1	HEI	(S)-OH $\rightarrow$ H	51	2.91 $\pm$ 0.03
2			51	2.82 $\pm$ 0.05
3			51	2.18 $\pm$ 0.06
4			51	2.84 $\pm$ 0.05
5			51	2.09 $\pm$ 0.01
6		(R)-OH $\rightarrow$ H	51	2.54 $\pm$ 0.04
7		Nle $\rightarrow$ Gly	51	0.39 $\pm$ 0.10
8			101	0.28 $\pm$ 0.02
9			80.8	-0.02 $\pm$ 0.01
10	MVT-101	Nle $\rightarrow$ Met	51	-2.81 $\pm$ 0.03

<sup>a</sup>In kcal/mol. The errors were obtained from the forward and backward values.

charges on the hydroxyethylene core, reduced peptide core, and Nle side chain determined in the above manner are given in Figures 5, 6, and 7, respectively. TIP3P parameters<sup>19</sup> were used for all water molecules.

The structure of the HIV-1 PR complexed with the inhibitor MVT-101 reported<sup>2</sup> as HVP4 in the Brookhaven protein data bank (pdb) was used in the present calculations. The inhibitor HEI was modeled in an extended conformation using the data given for MVT-101 and was docked into the active site of the enzyme by superimposing it on the MVT-101 structure. The overlap of the inhibitor HEI with MVT-101 is shown in Figure 8. The conformation of the modeled structure was found to be similar to the structures of the hydroxyethylene and the hydroxyethylamine inhibitors published later.<sup>4b,c</sup> The structure of the modeled enzyme-inhibitor complex around the inhibitor is shown in Figure 9. The modeled structure makes all the crucial interactions with the enzyme. Since this enzyme is active at around neutral pH, all the charged residues were left as charged except for a few which were involved in salt bridge interaction with neighboring oppositely charged residues. The amino and carboxyl termini of the two monomers of the enzyme were left as charged. Counterions were placed near the charged residues on the surface. In total 3 positively charged and 9 negatively charged ions were required. In the active site, one Asp residue (Asp-125 of the second strand) was made neutral and the other was left negatively charged. Some of the crystallographically determined water molecules found farther than 5 Å from the surface of the enzyme were discarded and the rest (about 70) were retained. This model system was solvated in a rectangular box (59.7  $\times$  46.3  $\times$  38.8 Å<sup>3</sup>) of 2056 water molecules. The total number of atoms in this system is about 7500.

The inhibitor, water, and counterion positions were initially minimized for 4000 cycles, next the enzyme was included for minimization for another 4000 cycles, which was followed by 100 cycles of minimization using SHAKE.<sup>20</sup> A 10-Å cutoff was used for the nonbonded interactions. A constant dielectric of 1 was used for all simulations. The system was initially equilibrated for 10.0 ps at constant temperature (300 K) using a time step of 0.001 ps. The whole inhibitor was treated as the perturbed group. The free energy perturbation calculations were carried out using the window method. In most simulations, the mutations were achieved in either 51 or 101 windows with 0.5 ps of equilibration and 0.5 ps of data collection at each window, which took 80–100 CPU hours on the Cray XMP/116.

The simulation for each mutation was repeated in water to determine the difference in the free energies of solvation and to complete the thermodynamic cycle described in Figure 4. For mutations in water, the inhibitors were placed at the center of a rectangular water box (45  $\times$  34

(11) Rao, B. G.; Singh, U. C. *J. Am. Chem. Soc.* **1991**, *113*, 6735.

(12) Tembe, B.; McCammon, J. A. *Comput. Chem.* **1982**, *8*, 281.

(13) Bash, P. A.; Singh, U. C.; Brown, F. K.; Langridge, R.; Kollman, P. A. *Science* **1987**, *235*, 574.

(14) Rao, S.; Singh, U. C.; Bash, P. A.; Kollman, P. A. *Nature* **1987**, *328*, 551.

(15) AMBER (Version 3.3) is a fully vectorized version of AMBER (Version 3.0): Singh, U. C.; Weiner, P. K.; Caldwell, J. W.; Kollman, P. A., University of California, San Francisco, 1986. AMBER (Version 3.3) also includes coordinate coupling and Intra/Inter decomposition.

(16) Weiner, S. J.; Kollman, P. A.; Case, D. A.; Singh, U. C.; Ghio, C.; Alagona, G.; Profeta, S.; Weiner, P. J. *Am. Chem. Soc.* **1984**, *106*, 765.

(17) QUEST (Version 1.0): Singh, U. C.; Kollman, P. A., University of California, San Francisco, 1986.

(18) Singh, U. C.; Kollman, P. A. *J. Comp. Chem.* **1984**, *5*, 129.

(19) Jorgensen, W. L.; Chandrasekhar, J.; Madura, J. D. *J. Chem. Phys.* **1983**, *79*, 926.

(20) Ryckaert, J. P.; Ciccoliti, G.; Berendsen, H. J. C. *J. Comput. Phys.* **1977**, *23*, 327.

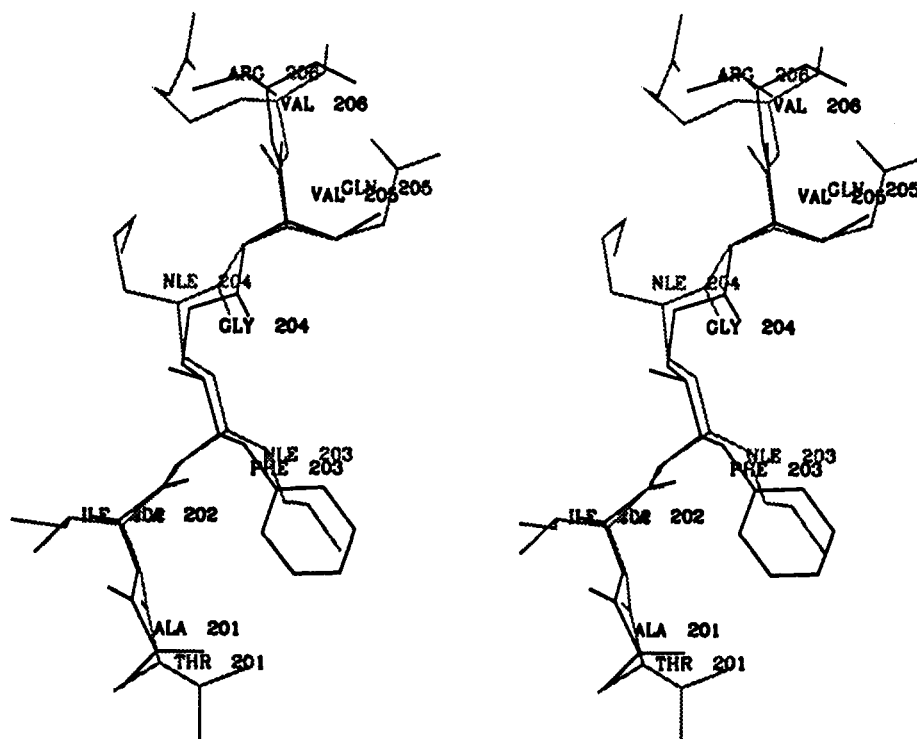


**Figure 8.** Superimposition of the HEI and MVT-101 inhibitors. The HEI is shown in dark lines. The residues of the inhibitor are numbered from 201 to 206.

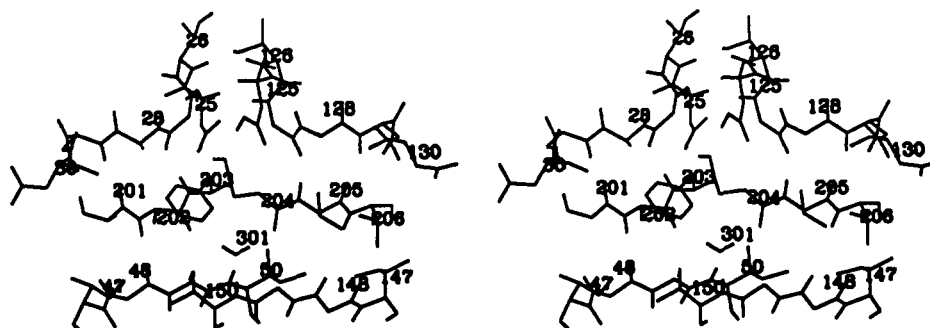


**Figure 9.** Structure of the enzyme-HEI complex around the inhibitor. The residues of the inhibitor are numbered from 201 to 206. Only the enzyme residues making direct hydrogen bonds with the inhibitor are shown. The flap water, WAT-301, is also shown. The residues are labeled by their residue numbers. These labels are omitted for clarity for some residues.

$\times 31 \text{ \AA}^3$ ) containing about 1460 water molecules. Each system (of about 4500 atoms) was minimized in four stages. First, the solvent around the solute was minimized for 500 cycles with the steepest descent method. Second, it was minimized for the next 2000 cycles with the conjugate gradient method. Third, the whole system was minimized with the conjugate gradient method for another 1000 cycles followed by a minimization of 100 cycles with SHAKE. Next the system was initially equilibrated for 10 ps at constant temperature (300 K) and pressure (1 atm) using a time step of 0.002 or 0.001 ps. During minimization, equilibration, and the subsequent perturbation runs, periodic boundary conditions were applied. A constant dielectric of 1 was used for all simulations. For nonbonded interactions, a cutoff distance of 10 Å was employed. The whole inhibitor was treated as the perturbed group. For each mutation, 51 or 101 windows were employed with 0.5 ps equilibration followed by 0.5 ps of data collection at each window, which took about 25 or 50 CPU hours on the Cray XMP/116.

## Results

**Mutations on the Inhibitors in Water.** The results of different mutations on the two inhibitors in water are given in Table I. All simulations except the last one involve the mutations on the inhibitor HEI. The last mutation is on the MVT-101 inhibitor. The first 5 simulations determine the free energy change for the mutation of the (*S*)-OH group of the inhibitor HEI to a hydrogen. This mutation was carried out with different simulation conditions to check the dependence of the calculated free energy changes on these conditions. These simulations were started from different

configurations of the inhibitor in water. The first three simulations were carried out at constant temperature (300 K) and constant pressure (1 atm) whereas the next two simulations were carried out at constant volume. Simulation 1, which used the most optimal GIBBS input parameters (see ref 11), gave a  $\Delta G_{\text{sol}}$  value of 2.91 kcal/mol. For simulation 2 with no cutoff for the nonbonded interactions between the inhibitor atoms, the calculated value is 2.82 kcal/mol, which is close to the earlier value. The removal of the periodic boundary conditions on the solute-solvent interactions in simulation 3 reduced the value to 2.18 kcal/mol. The constant volume simulations with two different starting configurations resulted in 2.84 and 2.09 kcal/mol for the same mutation. Some plausible reasons for the differences in these values were discussed in our earlier paper.<sup>11</sup> The mean of the above 5 values is 2.57 kcal/mol and the standard deviation is 0.40 kcal/mol. The two values are fairly close to the values obtained for a similar OH group mutation on pepstatin. The results show that the error in the calculated solvation free energy differences is about 15%.

Simulation 6 is on the mutation of the (*R*)-OH of the inhibitor HEI to a hydrogen. This mutation was carried out with the same GIBBS input as that used for simulation 1. The  $\Delta G_{\text{sol}}$  for this mutation is 2.54 kcal/mol, which is close to the value in simulation 1 and almost equal to the average value of the first five simulations. The results of these two mutations, therefore, suggest that there is no difference in the free energy of solvation of the two dia-

Table II. The Mutation Results on the Inhibitors Inside the Enzyme

no.	inhibitor	mutation	time, ps	$\Delta G_{\text{enz}}^a$
1	HEI	(S)-OH $\rightarrow$ H	51	3.63 $\pm$ 0.13
2			51	9.35 $\pm$ 0.10
3		(R)-OH $\rightarrow$ H	51	5.35 $\pm$ 0.03
4			51	5.20 $\pm$ 0.05
5			51	5.95 $\pm$ 0.10
6		Nle $\rightarrow$ Gly	51	1.88 $\pm$ 0.12
7	MVT-101	Nle $\rightarrow$ Met	51	-2.14 $\pm$ 0.02
8			51	-2.07 $\pm$ 0.02

<sup>a</sup>In kcal/mol. The errors were obtained from the forward and backward values.

stereomers of the inhibitor HEI.

Simulations 7, 8, and 9 are on the mutation of Gly at the P<sub>1</sub>' site of the inhibitor HEI to Nle. For sampling reasons, the mutation was carried out in the reverse direction. The starting structure of the modified inhibitor with Nle side chain at P<sub>1</sub>' was modeled such that the new side chain matches with the P<sub>1</sub>' side chain of MVT-101 when the two inhibitors were superimposed. The perturbation in these simulations is much larger than those in the simulations of the OH group mutations. Therefore, the mutation was carried out in three different ways each with a different total simulation time. In simulation 7, the mutation was carried out with 51 windows for 51 ps as in most other simulations. Simulation 8 doubled the number of windows to 101 and the total time to 101 ps. Simulation 9 was carried out with 40 windows for 80.8 ps using a time step of 0.002 ps instead of 0.001 ps. The free energy changes from the first two simulations 7 and 8 are small and positive (0.39 and 0.28 kcal/mol), whereas the free energy change from simulation 9 is close to zero (-0.02 kcal/mol). The sampling difficulties are known to cause large errors in simulations of large hydrophobic side chain mutations.<sup>21</sup> The mean of the three values is 0.22 kcal/mol with a standard deviation of 0.21 kcal/mol, suggesting that the solvation free energy difference between the two inhibitors is very small.

The last simulation, number 10, is on MVT-101 inhibitor and involves the mutation of Nle to Met at the P<sub>1</sub> and P<sub>1</sub>' positions. Unlike the earlier mutation, this one involves only a small change of a methylene group to a sulfur on the side chains. The  $\Delta G_{\text{sol}}$  for this mutation is -2.81 kcal/mol, which suggests that the Met-substituted MVT-101 is more soluble in water than the parent inhibitor.

**Mutations on the Inhibitors Inside the Enzyme.** In our earlier work<sup>11</sup> on pepstatin-*rhizopus* pepsin, we have pointed out that the two carboxyl side chains of the Asp diad do not remain coplanar during the equilibration and perturbation runs and the coplanar configuration is crucial for the optimal interaction between the enzyme and the inhibitor. The free energy differences obtained for some mutations were considerably affected by the distortion of the Asp diad configuration. The calculated values obtained with the constraints on the Asp diad (to keep it closer to coplanar configuration as in the crystal structure) were closer to the experimental binding affinity differences. The dynamics of the HIV-1 PR in water has been characterized in a recent molecular dynamics study, but no side chain motions have been analyzed.<sup>22</sup> In our simulations of the inhibitor complexes of HIV-1 PR, the planarity of the active site Asp carboxylates were found to be distorted in the same manner as described for *rhizopus* pepsin in our earlier study.<sup>11</sup> The distance constraints between four oxygens of the Asp diad carboxyl groups<sup>23</sup> have been applied to keep them in coplanar configuration observed in the crystal structure. The free energy simulations on the enzyme-inhibitor complexes were carried out both with and without the active site

constraints. The free energy differences obtained for different mutations on the two inhibitors complexed with the enzyme are given in Table II.

**Mutation of the (S)-OH Group.** Simulation 1 used no constraints on the active site and the resulting free energy change is 3.63 kcal/mol. For the same mutation with the active site constraints in simulation 2, a larger free energy difference of 9.35 kcal/mol was obtained. The large difference in the values obtained in the two simulations is due to the differences in the strengths of the interactions between the OH group and the Asp carboxylates. The OH group makes multiple interactions with the active site Asp carboxylate constrained in coplanar configuration, whereas it makes only one strong interaction with one of the outer oxygens of the Asp carboxylates in the distorted configuration. Interestingly, these two values are about 1.0 kcal/mol higher than the values obtained for a similar mutation of the OH group of pepstatin in the *rhizopus* pepsin active site. The lower values in *rhizopus* pepsin may be due to the lower basicity of the carboxyl groups due to the hydrogen bonding from the neighboring Thr/Ser side chain hydroxyls.

**Mutation of the (R)-OH Group.** For the mutation of the OH group in the *R* diastereomer of the inhibitor, the free energy change obtained without the active site constraints in simulation 3 is 5.35 kcal/mol, which is much larger than the value obtained in simulation 1. To make sure that this is not an artifact of the starting structure, the mutation was repeated with a different equilibrated starting structure in simulation 4 and a free energy change of 5.20 kcal/mol was obtained. This value is close to the previous value. For the same mutation with active site constraints in simulation 5, the obtained free energy difference is 5.95 kcal/mol, which is also close to the previous two values. For a similar mutation of the (R)-OH of pepstatin in *rhizopus* pepsin, the free energy changes obtained with and without the constraints were very close, but much smaller (about 3.0 kcal/mol) than the values obtained in this mutation of HIV-1 PR inhibitor. The near equal values obtained with or without constraints may be explained by the fact that the OH group placed in the *R* configuration makes only a single strong interaction with one of the outer oxygens of the Asp diad in either situation. The larger free energy change for this mutation may be due to the structural differences around the Asp diad. Higher basicity of the carboxylates of HIV-1 PR Asp diad may be responsible for stronger interaction with the inhibitor hydroxyl group.

**Mutation of the P<sub>1</sub>' Side Chain.** For the mutation of the Nle to Gly at the P<sub>1</sub>' site on inhibitor HEI in simulation 6, the free energy change is 1.88 kcal/mol. This simulation was carried with active site constraints and it was not repeated without the constraints.

**Mutation of Nle to Met on MVT-101.** Simulations 7 and 8 were on the mutation of Nle to Met on the MVT-101 inhibitor carried out with and without the constraints, respectively. The free energy differences from these two simulations are -2.14 and -2.07 kcal/mol. Obviously, the results are not affected for this mutation by differences in the configuration of the Asp carboxylates at the center of the active site. The site of this mutation is inside the S<sub>1</sub> and S<sub>1</sub>' binding pockets of the enzyme; the size and shape of these pockets do not appear to be affected by the distortions around the Asp diad. Therefore, it does not appear to be necessary to constrain the Asp configuration if the perturbations are carried out on the sites away from the central hydroxyl group of the inhibitor.

## Discussion

The  $\Delta\Delta G_{\text{bind}}$  values for different mutations were computed from the  $\Delta G_{\text{enz}}$  and  $\Delta G_{\text{sol}}$  values obtained in different simulations. These values are summarized in Table III. For each mutation, the  $\Delta G_{\text{sol}}$  values obtained in several mutations were averaged and the average values are presented in the table. The  $\Delta G_{\text{enz}}$  values obtained with or without constraints and those obtained with different starting structures are listed as different entries in this table.

The average free energy change for mutation of the central hydroxyl of the hydroxyethylene isostere inhibitor HEI to a hy-

(21) Merz, K. M.; Murcko, M. A.; Kollman, P. A. *J. Am. Chem. Soc.* **1991**, *113*, 4484.

(22) Swaminathan, S.; Harte, W. E.; Beveridge, D. L. *J. Am. Chem. Soc.* **1991**, *113*, 2717.

(23) The virtual bond is set up between two nonbonded atoms to constrain the distance between the two atoms to an initial distance. This is achieved by substituting the nonbonded interactions between the two atoms by a bond stretching term with a force constant of 200 kcal/Å. The interaction potential between the two atoms and the rest of the system is not affected.

Table III. The Calculated and the Experimental  $\Delta\Delta G_{\text{bind}}$  Values<sup>a</sup>

no.	inhibitor	mutation	$\Delta G_{\text{enz}}$	$\Delta G_{\text{sol}}$	$\Delta\Delta G_{\text{bind}}$	$\Delta\Delta G_{\text{expt}}$
1	HEI	(S)-OH $\rightarrow$ H	3.63 $\pm$ 0.13	2.57 $\pm$ 0.40	1.06 $\pm$ 0.53	
2			9.35 $\pm$ 0.10		6.78 $\pm$ 0.50	
3		(R)-OH $\rightarrow$ H	5.27 $\pm$ 0.08	2.54 $\pm$ 0.04	2.73 $\pm$ 0.12	
4			5.95 $\pm$ 0.10		3.41 $\pm$ 0.14	
5		(S)-OH $\rightarrow$ R-OH	-2.13 $\pm$ 0.21	0.03 $\pm$ 0.44	-2.16 $\pm$ 0.65	2.6
6			3.40 $\pm$ 0.20		3.37 $\pm$ 0.64	
7		Nle $\rightarrow$ Gly	1.88 $\pm$ 0.12	0.22 $\pm$ 0.21	1.66 $\pm$ 0.33	
8	MVT-101	Nle $\rightarrow$ Met	-2.14 $\pm$ 0.02	-2.81 $\pm$ 0.03	0.67 $\pm$ 0.05	
9			-2.07 $\pm$ 0.02		0.74 $\pm$ 0.05	

<sup>a</sup>All values are in kcal/mol. Data for simulations 2, 4, 6, 7, and 9 were obtained with constraints.

drogen in water,  $\Delta G_{\text{sol}}$ , is equal to 2.57 kcal/mol. For the same mutation inside the active site of the enzyme, the  $\Delta G_{\text{enz}}$  values with and without constraints are 3.63 and 9.35 kcal/mol, respectively. These two different values lead to  $\Delta\Delta G_{\text{bind}}$  values of 1.06 and 6.78 kcal/mol, respectively. The experimental value for this mutation on the inhibitor HEI is not available for direct comparison. However, the experimental values on some other series of inhibitors were reported<sup>24</sup> after we finished these simulations and the experimental data suggest that the hydroxyl group contributes about 5 to 6 kcal/mol to the free energy of binding. These experimental values are closer to the  $\Delta\Delta G_{\text{bind}}$  value obtained with the constraints. The  $\Delta G_{\text{enz}}$  values are about 1.5 kcal/mol larger than those for pepstatin hydroxyl group mutation in the active site of *rhizopus* pepsin, suggesting that the hydroxyl group of the inhibitor has stronger interaction with the Asp carboxylates of HIV-1 PR than those of pepsin. This is mostly due to the absence of the side chain hydroxyls (of residues 28 and 128) making hydrogen bonds with the outer oxygens of the Asp diad carboxyl groups. The value obtained without the constraints is smaller. The same observation was made in the study of pepstatin binding to *rhizopus* pepsin. Therefore, it is clear that the coplanar configuration of the Asp carboxyl groups is crucial for the optimal interaction with the hydroxyl group of the inhibitor in both classes of enzymes.

For the mutation of the hydroxyl group positioned in the *R* configuration, the average free energy change in water,  $\Delta G_{\text{sol}}$ , is equal to 2.54 kcal/mol. For the same mutation inside the active site of the enzyme, the  $\Delta G_{\text{enz}}$  values with and without constraints are 5.27 and 5.95 kcal/mol, respectively. The corresponding  $\Delta\Delta G_{\text{bind}}$  values are 2.73 and 3.41 kcal/mol. For this mutation also, no experimental value on the inhibitor HEI is available for direct comparison. However, the experimental data<sup>24</sup> suggest that the (*R*)-OH contributes about 1.5–3.5 kcal/mol to the free energy of binding. These values are also fairly close to the calculated values. An important aspect of these results is that the *R* diastereomer of the inhibitor is considerably more potent than the dehydroxy analogue which is in contrast to the results on pepstatin binding to pepsins. Both the experimental and calculated results suggest that both the *R* diastereomer and the dehydroxy analogue of pepstatin bind to pepsins with comparable affinities.<sup>11</sup> The HIV-1 PR active site appears to bind the inhibitor with much less stereospecificity than the pepsins. This is mostly due to the differences in the structure around the Asp diad discussed earlier.

The two sets of data on *S* and *R* diastereomers are added to obtain the free energy changes for the conversion of the *S* diastereomer to *R*. The  $\Delta G_{\text{sol}}$  for this conversion is close to 0 kcal/mol. The  $\Delta\Delta G_{\text{bind}}$  values obtained with and without constraints are -2.16 and 3.37 kcal/mol, respectively. The experimental value for this mutation is 2.6 kcal/mol, which is closer to the calculated value with constraints. This agreement is very encouraging. However, the value obtained without constraints suggests that the *R* diastereomer is more potent than the *S* diastereomer. It has been reported by Roberts et al.<sup>6</sup> and Rich et al.<sup>7</sup> that the *R* diastereomers of a few inhibitors bind to HIV-1 PR better than the *S* diastereomer. Though this may be due to

the differences in the binding modes of the inhibitors,<sup>7</sup> a clear and unambiguous explanation is not yet advanced. We are examining the binding interactions of these inhibitors in different modes to get insights into structural and energetic aspects using the present methodology. Nevertheless it is clear from the present study that the active site of the HIV-1 PR has much reduced binding specificity toward these inhibitor alcohols than the pepsins.

The results of the next mutation on the P'<sub>1</sub> side chain of the inhibitor suggest that the addition of Nle side chain enhances the binding of the inhibitor to HIV-1 PR by about 1.7 kcal/mol. The experimental data<sup>1,24</sup> for this mutation on the inhibitor HEI are not available for direct comparison. However, the experimental data on some other series of inhibitors suggest that the filling of the S'<sub>1</sub> site by a hydrophobic site chain contributes about 1–2 kcal/mol. The calculated values, therefore, appear to be a good estimate for this mutation. This prediction may be tested if the exact compounds used in these simulations are made and assayed against the HIV-1 PR.

For mutation of Nle to Met, the calculated  $\Delta\Delta G_{\text{bind}}$  value is 0.7 kcal/mol, suggesting that Nle may bind to HIV-1 PR marginally better than Met. For this mutation also, there are no experimental data for direct comparison. The calculated results suggest that it is easier to desolvate the Nle analogue than the Met analogue, and thereby Nle binds marginally better than Met.

## Conclusions

The calculated free energy differences for different mutations on the hydroxyethylene isostere inhibitor are in good agreement with the available experimental data. As in our earlier study on pepstatin-*rhizopus* pepsin, the coplanar configuration of the active site Asp carboxylates has been found to be crucial for its optimal interactions with the inhibitor hydroxyl group. The free energy values obtained with active site constraints (used to keep the Asp diad configuration closer to the experimental structure) are closer to the experimental values than the calculated values obtained without such constraints. These results show the importance of accurate and complete structural information for obtaining reliable free energy differences. The calculations correctly predict that the *R* diastereomer of this inhibitor binds considerably better than the dehydroxy analogue (ethylene isostere) of the inhibitor in contrast to the results on pepstatin binding to *rhizopus* pepsin. The smaller difference in the  $\Delta\Delta G_{\text{bind}}$  values between the *S* and *R* diastereomers of the HIV-1 PR inhibitors compared to pepsin or renin inhibitors is due to the higher affinity of the *R* diastereomer of HIV-1 PR inhibitor. These differences may be attributed to the structural differences between the two classes of enzymes around the Asp diad at the center of the active site. The Nle side chain at the P'<sub>1</sub> position on the hydroxyethylene isostere is predicted to contribute about 1.5 kcal/mol to the binding. The binding free energy difference between MVT-101 and modified MVT-101 with Met substitutions at the P<sub>1</sub> and P'<sub>1</sub> positions is very small.

**Acknowledgment.** All the calculations were carried out on the Cray XMP/116-se supercomputer at the Scripps Research Institute. We are grateful to Dr. Richard A. Lerner for providing the computational facilities and encouragement. This research is partially supported by grants from NIH (RO1-GM 39410) and Miles Inc.

(24) Rich, D. H.; Green, J.; Toth, M. V.; Marshall, G. R.; Kent, S. B. H. *J. Med. Chem.* 1990, 33, 1288.